Fluoroalkyl Radical Generation by Homolytic Bond Dissociation in Pentacarbonylmanganese Derivatives

Roberto Morales-Cerrada, Christophe Fliedel, Jean-Claude Daran, Florence Gayet, Vincent Ladmiral, Bruno Ameduri, Rinaldo Poli

Fluoroalkyl radical generation by homolytic bond dissociation in pentacarbonylmanganese derivatives

Roberto Morales-Cerrada,[a,b] Christophe Fliedel,[a] Jean-Claude Daran,[a] Florence Gayet,[a] Vincent Ladmiral,[b] Bruno Améduri,[b]* and Rinaldo Poli[a]*

Abstract: Thermal decarbonylation of the acyl compounds $[Mn(CO)_5(COR_F)]$ (R_F = CF_3, **1**; CHF_2, **2**; CH_2CF_3, **3**; CF_2CH_3, **4**) yields the corresponding alkyl derivatives $[Mn(CO)_5(R_F)]$ (R_F = CF_3, **5**; CHF_2, **6**; CH_2CF_3, **7**; CF_2CH_3, **8**). Compounds **3**, **4**, **7** and **8** have not been previously reported. All compounds, except **8** which could not be obtained in a pure state, were fully characterized by analytical and spectroscopic methods, as well as by single-crystal X-ray diffraction for **1**, **2**, **4**, **5**, **6** and **7**. The solution IR characterization in the CO stretching region, with the assistance of DFT calculations, has allowed the assignment of several weak bands to vibrations of the $[Mn(^{12}CO)_4(eq\text{-}^{13}CO)(R_F)]$ and $[Mn(^{12}CO)_4(ax\text{-}^{13}CO)(R_F)]$ isotopomers and a ranking of the R_F donor power in the order $CF_3 < CHF_2 < CH_2CF_3 \sim CF_2CH_3$. The homolytic Mn-$R_F$ bond cleavage in $[Mn(CO)_5(R_F)]$, carried out at various temperatures for compounds **5**, **6** and **7** under saturation conditions, with trapping of the generated R_F radicals by tris(trimethylsilyl)silane (TTMSS, 10 equiv), has yielded activation parameters $\Delta H^{\ddagger}$ and $\Delta S^{\ddagger}$ that are believed to represent close estimates of the homolytic bond dissociation thermodynamic parameters. The values ($\Delta H^{\ddagger}$ = 53.8 ± 3.5 (**5**), 46.3±1.6 (**6**), 50.6±0.8 (**7**) kcal/mol; $\Delta S^{\ddagger}$ = 66.0±9.5 (**5**), 55.8±4.7 (**6**), 65.4±2.2 (**7**) cal mol^{-1} K^{-1}) are in close agreement with the results of a recent DFT study (*J. Organomet. Chem.* **2018**, *864*, 12-18). The ability of these complexes to undergo homolytic Mn-R_F bond cleavage was further demonstrated by the observation that compound **5** (the member with the strongest Mn-R_F bond) initiates the radical polymerization of vinylidene fluoride (CH_2=CF_2, VDF), to produce poly(vinylidene fluoride) (PVDF) in good yields by either thermal (100 °C) or photochemical (UV or visible light) activation.

Introduction

Alkylpentacarbonylmanganese(I) are landmark compounds in organometallic chemistry, first prepared by Coffield in 1957[1] and studied as models for the ubiquitous "migratory insertion" reaction leading to acyl derivatives,[2] which is a fundamental step in many catalytic cycles.[3] Among them, those containing a fluoroalkyl group have received special attention because of their enhanced thermal stability. Contrary to simple alkylpentacarbonyl-manganese(I) compounds, which are readily accessible by nucleophilic substitution of the halide in R-X by $[Mn(CO)_5]^-$, the analogous derivatives with fluorine-containing alkyl ligands are not accessible in this manner because the inverted polarity of the C-X bond leads instead to the formation of $[(CO)_5MnX]$ with release of R_F^-, with $[Mn_2(CO)_{10}]$ and R_F-R_F resulting from further secondary reactions.[4] However, this obstacle can be overcome by carrying out the nucleophilic substitution on the acyl chloride, R_FCOCl, or the corresponding anhydride, to obtain an acyl intermediate $[(CO)_5Mn(COR_F)]$, which can then be thermally decarbonylated. Thus, trifluoroacetylpentacarbonylmanganese(I), $[(CO)_5Mn(COCF_3)]$, resulting from the addition of $Na[Mn(CO)_5]$ to either trifluoroacetyl chloride[5] or trifluoroacetic anhydride,[4] was used to access $[(CO)_5Mn(CF_3)]$. Other $[(CO)_5Mn(R_F)]$ complexes have also been reported with R_F = CFH_2,[6] CF_2H,[6] and C_nF_{2n+1} (n = 1-4, 6).[7]

These complexes do not appear to have found direct use in catalysis, whereas many other organomanganese complexes are now intensively investigated as precatalysts for various transformations such as hydrosilylation,[8] dehydrogenative coupling,[8c, 9] C-H[10] and C-F[11] activation, etc. However, the possible implication of alkylpentacarbonylmanganese(I) systems with fluorinated alkyl chains in reversible-deactivation radical polymerization (RDRP) has recently been mentioned in contributions by Asandei *et al.*,[12] who described a beneficial role of $[Mn_2(CO)_{10}]$ on the polymerization of vinylidene fluoride (VDF, CH_2=CF_2) by the iodine transfer polymerization (ITP) controlling method. In this polymerization technique, most of the chains at any given time reside in an iodine-capped dormant form, PVDF-I, and are reversibly reactivated by a rapid degenerative exchange with the active radical chains, PVDF$^{\bullet}$, which insures a controlled growth by the degenerative transfer protocol.[13]

The radical polymerization of VDF produces two different types of chain ends, head (H) and tail (T), following the regular head-to-tail (dominant) monomer addition (PVDF-$CH_2CF_2^{\bullet}$ or $PVDF_H^{\bullet}$) and the inverted head-to-head monomer addition (PVDF-$CF_2CH_2^{\bullet}$ or $PVDF_T^{\bullet}$), respectively. The proportion of inverted monomer additions is only 3.5-6% under typical polymerization conditions,[14] but this defect is sufficient to limit the efficiency of ITP because the $PVDF_T$-I dormant chains are less easily reactivated, accumulate during the polymerization so that the control is eventually lost.[15] Carrying out the polymerization in the presence of $[Mn_2(CO)_{10}]$ and under visible light irradiation led to the reactivation of both dormant species. This was attributed to the ability of $[(CO)_5Mn^{\bullet}]$, produced by photolytic Mn-Mn bond cleavage, to abstract an iodine atom from the dormant chain ends, including from the more recalcitrant $PVDF_T$-I, to form $[(CO)_5MnI]$ and regenerate the reactive radical chain.[12] In these contributions, the possible direct interaction between $[(CO)_5Mn^{\bullet}]$ and the growing radical chains, leading to the organometallic dormant species $[(CO)_5Mn(PVDF_H)]$ and $[(CO)_5Mn(PVDF_T)]$, was

[a] Mr. R. Morales Cerrada, Dr. C. Fliedel, Dr. J.-C. Daran, Dr. F. Gayet, Prof. R. Poli
CNRS, LCC (Laboratoire de Chimie de Coordination)
Université de Toulouse, UPS, INPT
205 route de Narbonne, BP 44099, F-31077 Toulouse Cedex 4, France.
E-mail: rinaldo.poli@lcc-toulouse.fr

[b] Mr. R. Morales Cerrada, Dr. V. Ladmiral, Dr. B. Améduri
ICGM
Univ Montpellier, CNRS, ENSCM
Place Eugène Bataillon, 34095 Montpellier, France.
E-mail: bruno.ameduri@enscm.fr

Supporting information for this article is given via a link at the end of the document

also mentioned. However, no evidence for the formation of these species was obtained and it was stated that, if formed, such species may be readily reactivated under the thermal (40 °C) and photochemical (visible light) operating conditions of the polymerization.

Given our interest in organometallic-mediated radical polymerization (OMRP)[16] and in the application of this method to the controlled polymerization of fluorinated monomers,[17] we were interested in probing the possible dissociative activation of the Mn-C bond in $[(CO)_5Mn(R_F)]$ under both thermal and photochemical conditions. A recent computational study of all possible fluorinated ethyl derivatives, $[(CO)_5Mn(CH_{2-n}F_nCH_{3-m}F_m)]$ (n = 0-2; m = 0-3),[18] predicts that the Mn^I-C bond dissociation enthalpies (BDEs) are in the 42-53.5 kcal/mol range, the value depending on the C^α and C^β F substitution. Thus, a thermal activation of these bonds to produce radicals under mild conditions appears unlikely. In order to learn more about the possible radical generation by Mn^I-C homolytic cleavage in $[(CO)_5Mn(R_F)]$, we have undertaken to experimentally measure the Mn-C BDE in these compounds. For this purpose, the previously described derivatives with $R_F = CF_3$ and CHF_2 have been used, as well as new compounds with $R_F = CH_2CF_3$ and CF_2CH_3, the synthesis and characterization of which is reported here for the first time. The two new compounds were targeted because they represent models of the putative head and tail dormant species resulting from the hypothetical chain trapping by $[(CO)_5Mn^\bullet]$. In addition, preliminary observations on the use of $[(CO)_5Mn(CF_3)]$ as initiator for the radical polymerization of VDF are reported here.

Results and Discussion

(a) Synthesis

The compounds used in this study are shown in Scheme 1. The acyl compounds **1** and **2** and the corresponding alkyl derivatives **5** and **6** were synthesized according to the literature procedure, with minor modifications (see below).[19] The new derivatives with $R_F = CH_2CF_3$ and CF_2CH_3 were obtained by a similar procedure, namely addition of *in-situ* generated $[Mn(CO)_5]^-$ to 3,3,3-trifluoropropanoyl chloride, CF_3CH_2COCl, and 2,2-difluoropropanoyl chloride, CH_3CF_2COCl, respectively, to yield the acyl derivatives **3** and **4**, which were then decarbonylated to the alkyl derivatives **7** and **8**. Both compounds with the CH_2CF_3 group (**3** and **7**) were isolated and fully characterized. The decarbonylation of **3** proceeded smoothly by heating at 70 °C and the alkyl product **7** was recovered in acceptable yields. It is to be noted that the more direct reaction between $[Mn(CO)_5]^-$ and CF_3CH_2I failed to produce **7**, giving instead a complex mixture, in which $[(CO)_5MnI]$ was a major component. Quite clearly, the presence of three F atoms on the β-C atom is sufficient to invert the polarity of the C-I bond. The decarbonylation of **4** was not successful under any of the employed conditions (different temperatures and with or without different solvents). The target product **8** was indeed formed, as indicated by the spectroscopic data (*vide infra*), but subsequently decomposed upon prolonged heating before completion of the acyl precursor decarbonylation. The best conditions found for this reaction are shown in the experimental section. The reason for this behavior is presumably the weaker homolytic Mn-C bond strength in **8**, as suggested by DFT calculations (see section on the homolytic bond strength determination below),[18] resulting in a competition between the rate of thermal decarbonylation leading from **4** to **8** and the rate of product decomposition. For all other synthesized compounds, the purification steps were found more effective, faster and higher-yielding if carried out by column chromatography rather than by sublimation as in most of the previous reports. Another minor change relative to the literature procedures is the use of the Na/K alloy to reduce $[Mn_2(CO)_{10}]$, yielding $[Mn(CO)_5]^-$ as the potassium salt,[20] rather than the more commonly employed sodium amalgam.[21]

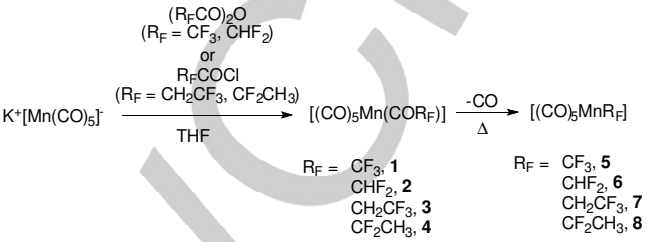

Scheme 1. Synthesis of pentacarbonylmanganese(I) compounds with fluoroalkyl groups.

Table 1. Selected ^1H, ^{19}F and ^{13}C NMR chemical shifts (δ) in acetone-d_6, with coupling constants in parentheses (in Hertz), for $[(CO)_5Mn(COR_F)]$ and $[(CO)_5Mn(R_F)]$ compounds.

R_F	^1H	^{19}F	^{13}C (C^α)	^{13}C (C^β)
		Acyl derivatives		
1	-	-81.9 s	115.0 q ($^1J_{CF}$ = 302)	-
2	5.24 t [a] ($^2J_{HF}$ = 57.8)	-119.2 d ($^2J_{FH}$ = 57.8)	111.5 dt ($^1J_{CF}$ = 256, $^1J_{CH}$ = 194)	-
3	4.05 q ($^3J_{HF}$ = 10.8)	-63.4 t ($^3J_{FH}$ = 10.8)	63.5 qt ($^2J_{CF}$ = 22.6, $^1J_{CH}$ = 131)	123.3 tq ($^1J_{CF}$ = 279, $^2J_{CH}$ = 6.7)
4	1.49 t ($^3J_{HF}$ = 19.3)	-91.5 q ($^3J_{FH}$ = 19.4)	117.9 tq ($^1J_{CF}$ = 250, $^2J_{CH}$ = 5.1)	17.0 qt ($^2J_{CF}$ = 26.1, $^1J_{CH}$ = 129.5)
		Alkyl derivatives		
5	-	5.65 s	153.3 q ($^1J_{CF}$ = 355)	-
6	7.46 t [b] ($^2J_{FH}$ = 48.6)	-71.6 d ($^2J_{FH}$ = 48.6)	143.8 dt ($^1J_{CF}$ = 287, $^1J_{CH}$ = 175)	-
7	1.40 q ($^3J_{HF}$ = 15.9)	-52.3 t ($^3J_{FH}$ = 16.9)	[c]	133.7 qt ($^1J_{CF}$ = 273, $^2J_{CH}$ = 6.0)
8	2.01 t [d] ($^3J_{HF}$ = 24.0 Hz)	-28.9 ($^3J_{FH}$ = 23.9)	[e]	[e]

[a] *Cf.* 4.85 ($^2J_{HF}$ = 59 Hz) in CCl_4.[6a] [b] Cf. 7.23 t ($^2J_{HF}$ = 48.5) in CCl_4.[6b] [c] Unidentified, perhaps overlapping with the strong solvent resonance. [d] Partially overlapping with the acetone-d_6 signal. Another NMR spectrum was carried out in benzene-d_6 to confirm the multiplicity of this peak (Figure S.A8.1). [e] Not available in sufficient amounts to record this spectrum.

(b) NMR characterization

The ^{1}H, ^{13}C and ^{19}F NMR spectra (shown in the SI, part A) reveal the expected chemical shifts and coupling patterns for all compounds, which are summarized in Table 1. The table also reports the full characterization of the derivatives with $R_F = CF_3$ and CHF_2. Curiously, although the latter are well-known compounds and have been analyzed by less routine techniques such as ^{55}Mn NMR[22] and XPS,[23] the more accessible properties shown in Table 1 have not all been previously reported to the best of our knowledge. The ^{1}H and ^{19}F NMR spectra show that, as expected, the two-bond fluorine-proton coupling constants ($^{2}J_{HF}$) are greater than the three-bond constants ($^{3}J_{HF}$). The latter value increases on going from the CH_2CF_3 to the CF_2CH_3 species and from the acyl to the alkyl species. On the other hand, the $^{2}J_{HF}$ for the CHF_2 derivatives is greater in the acyl one. In the ^{19}F NMR spectra, the chemical shifts for the CH_2CF_3 acyl and alkyl compounds are rather similar, with only a slight downfield shift after decarbonylation, whereas all compounds with F substitution on the α-C atom undergo a much greater downfield shift, as a consequence of direct coordination of the alkyl group to the metal atom. The ^{13}C spectra show all the expected $^{1}J_{CH}$, $^{2}J_{CH}$, $^{1}J_{CF}$ and $^{2}J_{CF}$, with $^{1}J_{CF} > {}^{1}J_{CH}$ in compounds **2** and **6**, $^{1}J_{CF} > {}^{2}J_{CF}$ and $^{1}J_{CH} > {}^{2}J_{CH}$. All these trends are as expected. The carbonyl region of the ^{13}C NMR spectra for compounds **1-4** (ca. 210 ppm) does not allow a clear distinction of the acyl carbonyl resonance, probably masked by the broad and stronger terminal Mn-CO resonances.

(c) X-ray diffraction studies

As stated above, the CF_3 and CHF_2 acyl and alkyl systems have been known for quite some time but have not been structurally characterized in the crystalline state. Indeed, X-ray diffraction studies of $[(CO)_5Mn(COR)]$ and $[(CO)_5MnR]$ compounds are quite limited and do not include any example of fluorine-containing carbyl ligand bonded to Mn *via* an sp^3-hybridized C atom. On the other hand, there are a few $[(CO)_5MnR]$ structures with F-containing groups bonded *via* an sp^2-hybridized C atom.[24] We have now determined the structures of the acyl compounds **1** and **2** and the corresponding alkyl compounds **5** and **6**, as well as those of the new acyl derivative **4** and the new alkyl derivative **7**. Views of the three acyl derivatives **1**, **2** and **4** are shown in Figure 1, while those of the alkyl derivatives **5**, **6** and **7** are given in Figure 2. Selected bond distances and angles are collected in Table 2 and more extensive metric data are given in the SI (part B). Of particular interest are the Mn-C distances to the R_F groups for the three alkyl complexes **5**, **6** and **7**, because the homolytic bond strengths to these alkyl groups have been predicted to be greater than in the non-F-substituted analogues.[18] For the structure of compound **6**, the molecule sits on a crystallographic mirror plane that imposes a symmetry disorder between the CHF_2 group and one of its *cis* CO ligands; a symmetry lowering did not provide a better crystallographic solution. Therefore, the parameters related to the two disordered groups are unreliable. In the better determined distance in **5**, with three α-F substituents, the Mn-CF_3 distance (2.067(3) Å) is ca. 0.1 Å shorter than that to the Mn-CH_2CF_3 distance in **7**, 2.162(2) Å. For comparison, other distances to sp^3-hybridized C atoms without any F substituents are 2.214(3) Å in $[(CO)_5Mn(CH_2CH{=}CHCOOPh)]$[25] and 2.195(6) and 2.196(8) Å in $[(CO)_5Mn(CH_2CH_2\text{-}o\text{-}C_6H_4\text{-}CH_2CH_2)Mn(CO)_5]$,[26] whereas positional disorder in the simpler reference compound $[(CO)_5Mn(CH_3)]$ prevented an accurate determination of the Mn-CH_3 distance.[27] The distance in $[(CO)_5Mn(CH_2Cl)]$, with one α-Cl substituent, is 2.125(10) Å.[28] These data suggest that electronegative substituents (particularly F, but even Cl), even when placed on the β-C atom as in **7**, strengthen the Mn-C bond, in agreement with the recent DFT study.[18]

Table 2. Selected bond distances (in Å) from the X-ray structures of $[(CO)_5Mn(COR_F)]$ and $[(CO)_5Mn(R_F)]$.

Parameter	Acyl compounds		
	1	**2**	**4**
Mn-C (COR_F)	2.051(3)	2.057(5)	2.0748(14)
Mn-CO_{trans}	1.869(3)	1.869(6)	1.8562(15)
Mn-CO_{cis}	1.872(3) 1.862(3) 1.863(3) 1.879(3)	1.875(6) 1.880(6) 1.862(5) 1.858(6)	1.8809(14) 1.8617(14) 1.8566(14) 1.8697(14)
Parameter	Alkyl compounds		
	5	**6**	**7** [a]
Mn-C (R_F)	2.067(3)	1.971(2) [b]	2.167(2)/2.162(2)
Mn-CO_{trans}	1.858(3)	1.861(2) [b]	1.834(2)/1.842(2)
Mn-CO_{cis}	1.872(2) 1.873(2)	1.853(3) 1.859(3)	1.871(2)/1.870(2) 1.860(2)/1.865(2) 1.869(2)/1.868(2) 1.870(2)/1.869(2)

[a] Values for two independent molecules in the asymmetric unit. [b] Unreliable parameter because of symmetry-related disorder.

(d) Infrared characterization

The infrared analysis in the Mn-CO stretching region has revealed unprecedented features. Table 3 collects the relevant data and also compares the measured frequencies with those already reported in the literature for the already known compounds (**1**, **2**, **5** and **6**). The spectra are shown in the SI (part C). Compound **8** could not be obtained in sufficiently pure form to record a reliable IR spectrum. The frequency trend indicates that the alkyl donor power varies in the increasing order $CF_3 < CHF_2 < CH_2CF_3$. The placement of the CF_2CH_3 derivative in this series is ambiguous because of the attenuated effect in the series of acyl derivatives (**1-4**). The Mn-CO frequencies in the $COCF_2CH_3$ complex **4** appear rather similar to those in the $COCHF_2$ complex **2**. The presence of additional bands relative to the three ones ($2A_1$+E) expected for the $(CO)_5Mn$ moiety in ideal C_{4v} symmetry is related to symmetry lowering, resulting in E band splitting and in the appearance of the "forbidden" and therefore weak B_1 band. In addition, rotational isomerism results in the appearance of a second –COR vibration for the acyl derivatives.[6] Additional weak bands are also observed in the Mn-CO stretching region (see Table 3). A few of these were also previously observed for the alkyl compounds **5** and **6** and attributed to ^{13}C-containing isotopomers,[6b] but a detailed symmetry analysis has not been previously carried out. These bands cannot originate from by-products that contain the fluoroalkyl groups because the compounds are spectroscopically pure (^{1}H, ^{13}C, ^{19}F NMR, SI part A). Their assignment to by-products that do not contain the fluoroalkyl group is also unlikely because the frequencies depend on the nature of this group.

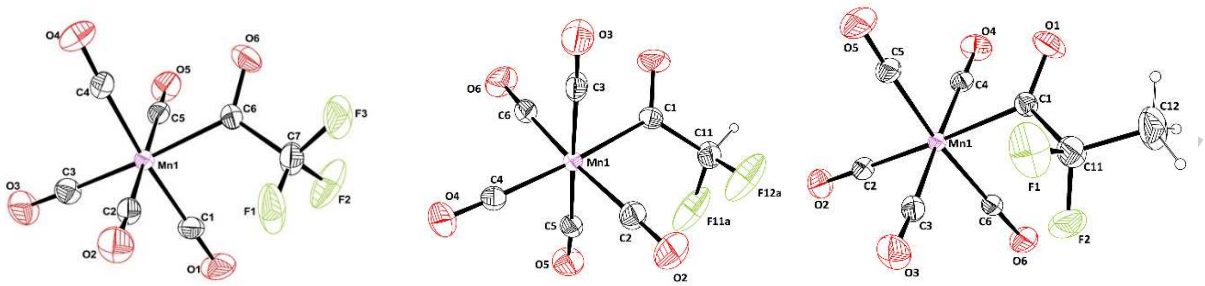

Figure 1. ORTEP views of the acyl compounds **1** (left), **2** (centre) and **4** (right). Thermal ellipsoids are drawn at the 50 % level.

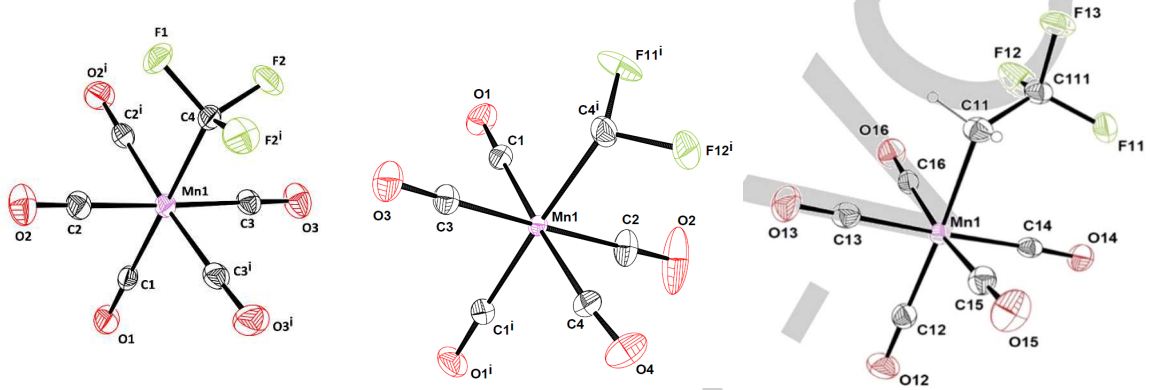

Figure 2. ORTEP views of the alkyl compounds **5** (left), **6** (center) and **7** (right). For the structure of **6**, only one of the two symmetry-equivalent orientations of the C1 and C4 atoms is presented for clarity. Thermal ellipsoids are drawn at the 50 % level.

Table 3. IR vibrations of $[(CO)_5Mn(COR_F)]$ and $[(CO)_5Mn(R_F)]$ compounds in the CO stretching region.

R_F	Solvent									Reference
Acyl derivatives		A_1	B_1	E	A_1	A_1 (*eq.* ^{13}C)	$E_{(2)}$ (*eq.* ^{13}C)	A_1 (*ax.* ^{13}C)	acyl	
1	pentane	2131 w	2070 w	2039 vs	2023 s	2001 w	1981 vw	1944 vw	1722 vw, 1665 w	This work [a]
2	pentane	2125 w	2062 w	2036 s, 2028 s	2015 s	-	-	-	1658 w, 1643 w	[6a]
	pentane	2127 w	2063 w	2038 vs, 2031 vs	2017 s	1997 w	1975 vw	1938 vw	1660 w, 1645 w	This work
3	pentane	2122 w	2063 w	2028 s, 2020 vs	2012 s	1975 vw	-	1940 vw	1663 w, 1652 w	This work
4	pentane	2125 w	2061 w	2037 vs, 2028 vs	2014 s	1994 w	1972 vw	1936 vw	1663 m, 1615 vw	This work
Alkyl derivatives		A_1	B_1	E	A_1		E(2) (eq. ^{13}C)	A1 (ax. ^{13}C)		
5	pentane	2137 w [b]	2075 vw [c]	2045 vs	2021 s	2010 w	1978 vw	1940 vw	-	This work
	heptane	2136 w	2068 sh	2044 vs	2019 s	2007 w	1977 vw	-	-	[6b]
	cyclohexane	2134.5	(2072) [d]	2043.4	2019.5	-	-	-	-	[29]
6	pentane	2128 w	2064 w	2031 vs	2011 s	1984 sh	1970 vw	1930 vw	-	This work
	heptane	2127 w	2062 w 2044 sh	2029 vs	2010 s	1982 w	1968 vw	-	-	[6b]
7	pentane	2124 w	2062 w	2030 vs	2004 s	ca. 1990 sh	1962 vw	1930 vw	-	This work

[a] Cf. 2139 w-m, 2035 vs, 2002 m(sh), 1643 m-s in KBr pellet.[4] [b] Shoulder (vw) at 2127 assigned to the A_1 band of the *eq*-^{13}C isotopomer. [c] A second weak band at 2066 cm^{-1} is assigned to the B_1 vibration of the *eq*-^{13}C isotopomer, see text and Figure 4. [d] Value obtained from the Raman spectrum.

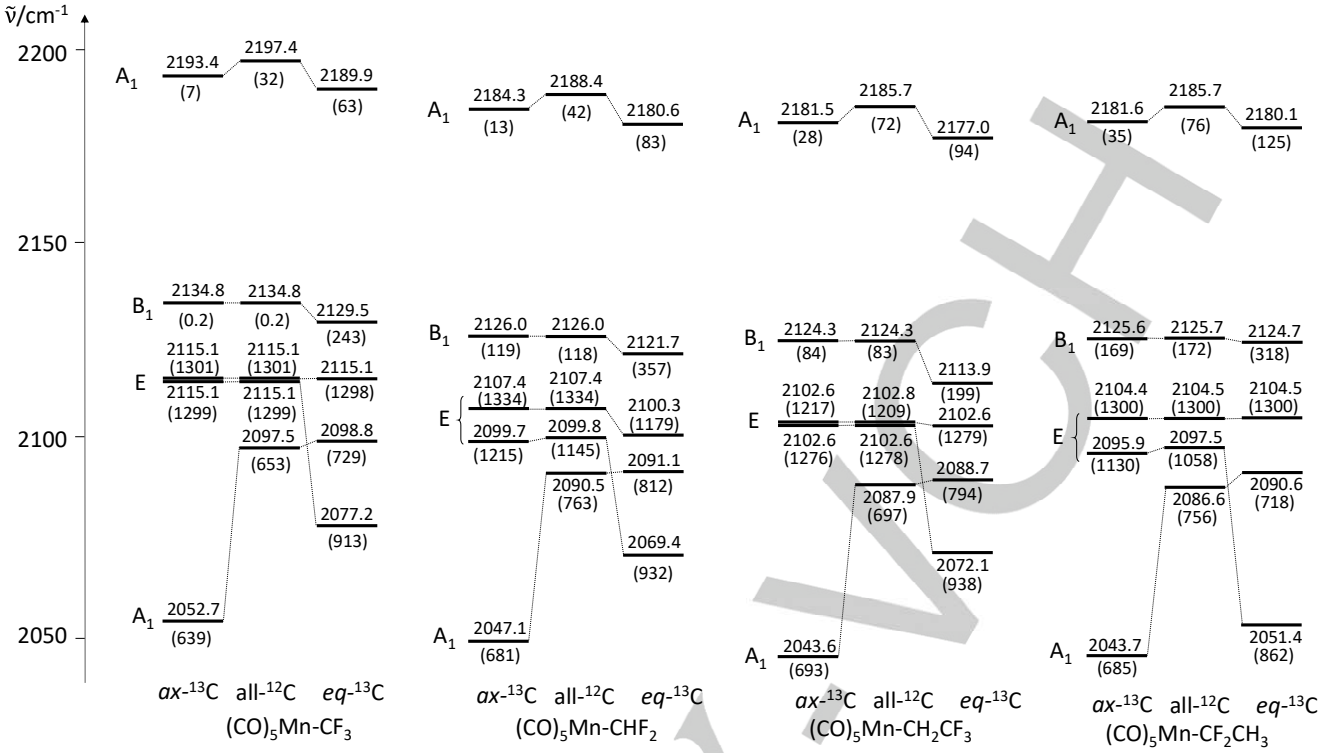

Figure 3: DFT-calculated terminal Mn-CO stretching frequencies (in cm^{-1}) and relative intensities (in parentheses) for the $(CO)_5MnR_F$ complexes **5** ($R_F = CF_3$), **6** ($R_F = CHF_2$), **7** ($R_F = CH_2CF_3$) and **8** ($R_F = CF_2CH_3$).

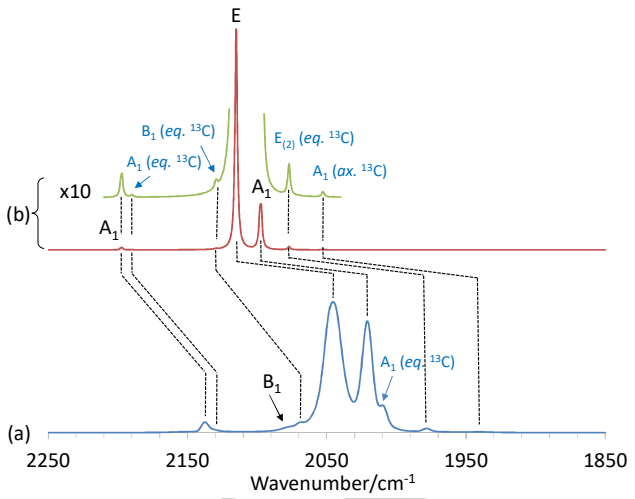

Figure 4. Experimental (a) and DFT-calculated (b) IR spectra of compound **5** in the terminal carbonyl stretching region. For the calculated spectrum, the bands are reported as Lorentzian functions with 2 cm^{-1} half-height width and relative intensities as indicated by the calculations. The spectra of the [$(^{12}CO)_5Mn(CF_3)$], [(*eq*-^{13}CO)($^{12}CO)_4Mn(CF_3)$] and [(*ax*-^{13}CO)($^{12}CO)_4Mn(CF_3)$] isotopomers were summed up with relative contributions calculated from the ^{13}C natural abundance and the isotopomers with double (or more) ^{13}C substitution were neglected.

A full frequency analysis was carried out by DFT calculations for all alkyl complexes (**5**-**8**). A summary of the calculated frequencies is shown in Figure 3 and a comparison of the DFT-calculated and the experimental IR spectrum for the representative compound **5** is illustrated in Figure 4. Analogous comparisons for compounds **6** and **7** are reported in the SI (part D). The calculated spectrum is shifted to higher wavenumbers relative to the experimental one, which is a common phenomenon for DFT-calculated IR spectra, but the general shape of the spectrum is reproduced quite well. The calculations confirm the relative order of alkyl donor power established from the experimental spectra (see above) and allow assessing the donor power of the CF_2CH_3 substituent in **8** as being relatively similar to that of the CH_2CF_3 substituent in **7** (the frequency changes are small and of opposite sign for bands of different symmetry type). The calculations not only confirm the previous assignment of the main (all-^{12}C) isotopomer bands for compounds **5** and **6**,[6, 29] but also allowed clear identification and assignment of a few weak bands related to the ^{13}C-containing isotopomers.

Three weak bands are visible on the low frequency side of the last band (A_1) of the main isotopomer. One results from the significant shift of one of the two E-type bands for the isomer with equatorial ^{13}C. A second one (not previously reported) is the lower-energy A_1 band for the isotopomer with axial ^{13}C. The assignment of the last one of these three bands, which is clearly visible at 2010 cm^{-1} for **5** (see Figure 4) but only as a shoulder of the stronger A_1 band for **6** and **7** (Figures S.D.1 and S.S.2), is less straightforward. On the basis of our DFT analysis (Figure 3), the only band that could appear in this region is the *eq*-^{13}C isotopomer lower-frequency A_1 vibration and we therefore tentatively assign it to this vibrational mode. However, the calculations predict a blue-shift upon isotopic substitution. This outcome may originate from an altered mixing of the Mn-CO vibrators in the two A_1 normal modes, whereas the mere isotopic substitution should lead to a red-shift.

Possibly, the actual situation in *n*-pentane solution is different than in the gas phase and indeed results in the expected red-shift.

A shoulder on the low-frequency side of the high-frequency A_1 band, which is visible for all three compounds, seems attributable to the corresponding A_1 vibration of the *eq*-^{13}C isotopomer. The weak band at 2066 cm^{-1} for compound **5**, slightly blue-shifted from the strongest E band of the main isotopomer, is assigned to the *eq*-^{13}C isotopomer B_1 mode. This band gains in intensity relative to the corresponding one of the main isotopomer (243 relative to 0.2, see Figure 3) because the vibrator local C_{4v} symmetry is broken by the isotopic substitution. The weaker and further blue-shifted band in the experimental spectrum (shoulder at ca. 2080 cm^{-1}) is tentatively attributed to the B_1 vibration, possibly gaining intensity relative to the gas-phase calculated spectrum by dynamic symmetry breaking resulting from solvation. For the other two alkyl derivatives **6** and **7**, the lower symmetry of the alkyl group renders the B_1 band more intense and clearly visible, as shown in both the experimental and calculated spectra (see SI), while that of the *eq*-^{13}C isotopomer is hidden underneath the stronger B_1 and E bands of the main isotopomer. All other calculated bands of the *eq*-^{13}C and *ax*-^{13}C isotopomers overlap with the stronger bands of the main all-^{12}C component.

(e) Determination of the activation barrier for the homolytic Mn-R_F bond cleavage

This study was only carried out for compounds **5**, **6** and **7**, because compound **8** could not be obtained in sufficient quantities and in a sufficiently pure state. Under thermal activation at constant temperature, the residual [$(CO)_5Mn(R_F)$] concentration was monitored by ^{19}F NMR spectroscopy in the presence of hexafluorobenzene as internal standard plus a large amount of a radical trapping agent (T, see Scheme 2), sufficient to insure saturation kinetics (reaction rate limited by the bond cleavage step and a first order decay, $-d[(CO)_5Mn(R_F)]/dt = k_a[(CO)_5Mn(R_F)]$). The same protocol was previously employed for the measurement of activation barriers for other radical-generating reactions, for instance the homolytic splitting of metal-metal bonds,[30] the Co^{III}-R cleavage in vitamin B12[31] and related model compounds,[32] or the alkyl halide activation by metal catalysts in atom transfer radical polymerization systems.[33] For the metal-metal and metal-carbon breaking processes, where the reverse reaction is presumed to have a very small activation barrier, the kinetic activation enthalpy was considered as a good upper-limit approximation of the thermodynamic bond dissociation enthalpy (BDE). An important difference between the present system and the above-cited precedents is that the co-product of the organic radical (equation 1), namely [$(CO)_5Mn^{\bullet}$], is itself a reactive radical. In addition to efficiently trapping the $R_F^{\bullet}$ radical in equation 2 ($k_{trap,R}[T] >> k_{da}[(CO)_5Mn^{\bullet}]$), the trapping agent T may also possess the ability to efficiently trap the [$(CO)_5Mn^{\bullet}$] radical (equation 3a) ($k_{trap,Mn}[T] >> k_{da}[R_F^{\bullet}]$). It is also known from flash photolysis studies that the bimolecular coupling of the [$(CO)_5Mn^{\bullet}$] radicals (equation 3b) is an extremely fast process ($k_{dim} = 1.9\cdot10^9$ M^{-1}s^{-1}).[34] It has to be mentioned here that the BDE of the Mn-C bond in compounds **5** and **6** has also been indirectly estimated by Calvet calorimetry[35] and by photoionization mass spectrometry.[36]

The selection of an appropriate trapping agent is of key importance. A successful trapping agent must not only react rapidly and irreversibly with R_F (and possibly also with [$(CO)_5Mn^{\bullet}$]); it must also be inert relative to the starting compound [$(CO)_5Mn(R_F)$] under the thermal degradation conditions. We initially considered TEMPO, since this compound was used in several of the above-mentioned radical trapping studies. However, preliminary experiments carried out on compound **7** did not lead to the formation of the expected TEMPO-CH_2CF_3 product (^{19}F NMR signal reported at δ -71.58 in $CDCl_3$)[37] and did not reveal the expected simple kinetic behavior (details in the SI, part E.1). A potential problem is the action of TEMPO as a ligand.[38] Coordination to Mn^{I} may occur at a site left vacant by CO dissociation or by migratory insertion, followed by degradation by a pathway that does not involve Mn-C bond cleavage as the initial step. Our attention was therefore turned toward tris(trimethylsilyl)silane, $(TMS)_3SiH$ (TTMSS), since this molecule can be reasonably expected to display poorer coordinating properties than TEMPO. It has been extensively used as a radical-based reducing agent[39] and as an efficient H atom donor to a variety of carbon-centered radicals $R^{\bullet}$.[40] It has also been shown that the $(Me_3Si)_3Si^{\bullet}$ radical generated by H atom transfer dimerizes to $Si_2(SiMe_3)_6$.[41] Furthermore, $Si_2(SiMe_3)_6$ is known to react with [$Mn_2(CO)_{10}$] to produce [$(CO)_5MnSi(SiMe_3)_3$] with liberation of H_2.[42] The use of the related Me_3SiH to trap CH_3 radicals thermally generated from [$Mn(CO)_5(CH_3)$] has previously been described, although that investigation did not assess the barrier to the homolytic bond cleavage.[43]

$$[(CO)_5Mn\text{-}R_F] \underset{k_{da}}{\overset{k_a}{\rightleftharpoons}} [(CO)_5Mn]^{\bullet} + R_F^{\bullet} \quad (1)$$

$$R_F^{\bullet} + T \xrightarrow{k_{trap,R}} \text{trapped product} \quad (2)$$

$$[(CO)_5Mn]^{\bullet} + T \xrightarrow{k_{trap,Mn}} \text{trapped product} \quad (3a)$$

$$2\,[(CO)_5Mn]^{\bullet} \xrightarrow{k_{dim}} [Mn_2(CO)_{10}] \quad (3b)$$

Scheme 2. Thermal decomposition of (fluoro)alkylpentacarbonylmanganese(I) compounds in presence of a radical trap.

Table 4. Kinetics and activation parameters for the decay of compounds **5**, **6** and **7** in C_6D_6.

	T/°C	k_a/s^{-1}	$\Delta H^{\ddagger}$/kcal mol^{-1}		$\Delta S^{\ddagger}$/cal mol^{-1} K^{-1}	
			Exp.	DFT [a]	Exp.	DFT [a]
	100	$(3.10\pm0.18)\cdot10^{-4}$				
5	95	$(1.04\pm0.06)\cdot10^{-4}$	(53.8 ±3.5) [b]	55.1	(66.0±9.5)	45.8
	90	$(4.08\pm0.29)\cdot10^{-5}$				
	85	$(6.27\pm0.33)\cdot10^{-4}$				
6	80	$(2.51\pm0.08)\cdot10^{-4}$	(46.3±1.6) [c]	48.0	(55.8±4.7)	43.2
	75	$(9.40\pm0.13)\cdot10^{-5}$				
	90	$(5.35\pm0.07)\cdot10^{-4}$				
7	80	$(7.84\pm0.47)\cdot10^{-5}$	(50.6±0.8)	50.5	(65.4±2.2)	48.8
	70	$(8.52\pm0.41)\cdot10^{-6}$				

[a] Values from ref. [18]. [b] Reported as 48.5±1.4 kcal/mol by Calvet calorimetry[35] after re-evaluation,[36] and as 43.5±2.6 kcal/mol by photoionization mass spectrometry.[36] [c] Reported as 34.4±2.6 kcal/mol by photoionization mass spectrometry.[36]

Initial experiments, carried out on compound **5** at 100 °C in C_6D_6 as solvent with variable [TTMSS]/[Mn] ratio, revealed that a 10-fold excess of the silane is sufficient to insure saturation conditions ([TTMSS]-independent observed pseudo-first order rate constant), see SI (part E2) for details. The ^{19}F NMR monitoring allowed to derive the manganese complex decomposition kinetics (Figure S.E2.2) and gave unambiguous evidence for the production of CHF_3 (Figure S.E2.3), although detection of this product was made difficult by its extensive escape toward the tube head space (b.p. = -82.1 °C, low solubility in C_6D_6). Hence, all subsequent experiments were carried out with a 10-fold excess of TTMSS, see results in Table 4. All the first order decay plots are available in the SI (part E3). The Eyring analysis of the decay rate constants (Figure 5) provided the activation parameters that are also reported in Table 4. Note that the activation enthalpies obtained from the present study are greater than the thermodynamic bond dissociation enthalpies (BDEs) determined by Calvet calorimetry or by photoionization mass spectrometry,[35-36] see footnotes in Table 4. This discrepancy might result from an overestimation of the BDEs by the kinetic approach but, as argued above, the reverse bond formation process should proceed via a very low activation barrier, thus $\Delta H^{\ddagger} \approx$ BDE. The BDEs estimated by recent DFT calculations[18] are in much closer agreement with the $\Delta H^{\ddagger}$ values determined by the present study. It is also worth underlining that the activation entropies obtained from the Eyring analyses of the rate data are high and positive, also in relatively good agreement with the values obtained by DFT calculation for the full bond breaking process. Note that other calculations of the Mn-C bond strength for compounds **5** and **6**, carried out at a slightly different level of theory by Folga and Ziegler,[44] also gave high values in close agreement with those of the more recent DFT study and these authors concluded that the experimental estimates of the Mn-C BDEs available at that time were too low.

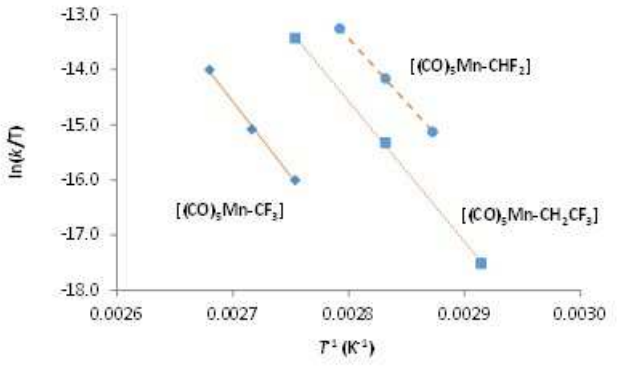

Figure 5. Eyring plots of k_{obs} as a function of temperature for the decomposition of compounds **5**, **6** and **7**.

In view of the forcing conditions used for this study, it is reasonable to question the existence of competing processes. Indeed, alkylpentacarbonylmanganese(I) derivatives are known to be prone to thermally activated migratory insertion and decarbonylation processes. These would generate vacant coordination sites opening access to other reaction pathways such as α- and β-elimination processes of atoms (H, F) from the alkyl chain. However, compounds **5-7** were found thermally stable in the absence of TTMSS. The interactions of silane with the reaction intermediates generated by migratory insertion and by decarbonylation have been investigated *in silico*, confirming that the homolytic cleavage pathway is the preferred one. These results will be reported separately in a forthcoming contribution. Finally, we point out that the calculated BDE for compound **8** (46.0 kcal mol^{-1}),[18] is slightly lower than those of the other three compounds, possibly rationalizing the failure to obtain this product by clean decarbonylation of **4** as suggested above in section (a).

(f) VDF polymerization with compound 5

Preliminary investigations of the radical generation from these fluoroalkyl derivatives of pentacarbonylmanganese(I) were carried out using compound **5**, which is the member of the series with the homolytically strongest bond according to both the experimental and the computational evidence, as an initiator for the polymerization of VDF. Full investigations of these complexes as radical polymerization initiators will be reported separately in a specialized polymer journal. The experiments were carried out in dimethyl carbonate under different conditions, see Table 5: thermal activation (entries 1 and 2), visible light at 40 °C (entry 3) and UV (300 nm) irradiation at 50 °C (entry 4), using a molar ratio [VDF]/[**5**] = 50.

Table 5. Yields, molar masses and dispersities (obtained by SEC using PMMA standards) of PVDF prepared by the radical polymerization of VDF initiated by compound **5**.[a]

Entry	Activ. method	T (°C)	Yield (%)	M_n (g·mol^{-1})	Đ
1	Thermal	50	0	-	-
2	Thermal	100	68	16,900	1.53
3	Visible light	40	60	40,300	1.47
4	UV light	50	74	24,800	1.54

[a] ≈ 1.5 g of VDF in 5 mL of dimethyl carbonate solution, V_{tot} ≈ 12 mL, 24 h.

Indeed, these processes led to the formation of polymer in high yields (≥60%) after 24 h, except when the thermal activation was carried out at 50 °C without irradiation (entry 1). After precipitation, the recovered product was proven to correspond to PVDF by ^1H and ^{19}F NMR spectroscopic analyses (SI, part F). The NMR solutions were clear, indicating the absence of inorganic metal impurities. The ^1H NMR spectra (Figures S.F.1, S.F.3 and S.F.5 for the products of thermal, visible and UV activation experiments) confirm the presence of both normal head-to-tail (HT) and inverted tail-to-tail (TT) dyads with characteristic signals located at 2.8-3.2 and 2.4 ppm, respectively.[12a, 13c, 45] Chain-end signals, assigned to PVDF-CF_2-CH_3 and PVDF-CH_2-CF_2H, respectively, are also observed at 1.9 and 6.3 ppm.[45-46] These signals result from chain transfer by the strong head and tail radicals to the solvent or monomer or from backbiting.[46a] The corresponding ^{19}F NMR spectra (Figures S.F.2, S.F.4 and S.F.6) display a major signal centered at -92 ppm for the regular head-to-tail dyads and lower intensity signals at -114.6 and -117.0 ppm, resulting from the HH addition, and a doublet of multiplets centered at -115.5

ppm assigned to CF_2H end-group in PVDF-CH_2-CF_2H.[12a, 13c, 45] In addition, small signals centered at -115.1 and -116.6 ppm might be attributed to the β and γ CF_2 groups relative to the manganese atom in PVDF-CH_2CF_2-CF_2CH_2-$Mn(CO)_5$, respectively.

The SEC analysis (Figure 6) reveals monomodal and relatively narrow MW distributions, which can be considered relatively narrow because a PVDF made under similar conditions (73 °C in dimethyl carbonate) by free radical polymerization showed, as expected, a dispersity value (*Đ*) of 2.1. The highest molar mass product was obtained from the visible light activation experiment and the lowest one from the thermal activation experiment. These molar masses are overestimated because of the use of PMMA standards. However, the dispersities are similar for all products. The negative signal in the size exclusion chromatogram results from the lower refractive index of PVDF relative to the DMF eluent.[46b-d]

Control experiments carried out with $[Mn_2(CO)_{10}]$ instead of complex **5** did not yield any PVDF. Since $[Mn_2(CO)_{10}]$ is known to generate $[(CO)_5Mn^{\bullet}]$ under both thermal and photochemical conditions, it can be concluded that the free $[(CO)_5Mn^{\bullet}]$ radicals are not capable to add onto VDF to initiate the polymerization. These results confirm previous studies by Bamford *et al.*[47] and by Asandei *et al.*,[12a] where $[(CO)_5Mn^{\bullet}]$ photoproduced from $[Mn_2(CO)_{10}]$ was shown unable to initiate the radical polymerization of VDF (although it does initiate those of C_2F_4 and C_2F_3Cl).

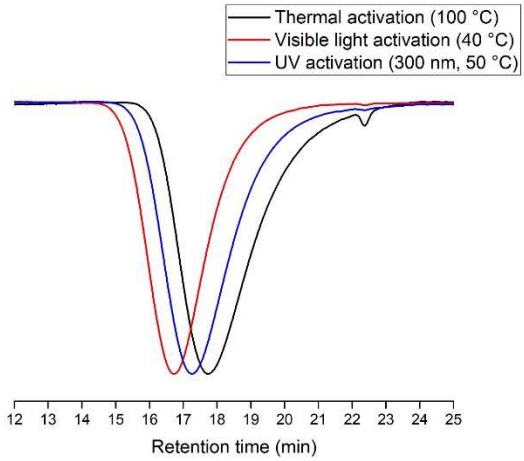

Figure 6. SEC traces of PVDF (entries 2, 3 and 4 in Table 5) in DMF.

Since VDF is known to polymerize only by the radical mechanism, the above results constitute proof of the generation of radicals by thermal decomposition of **5**. The major primary radical generated by this process, as shown above, is $CF_3^{\bullet}$. This radical is known to selectively add to the tail end of VDF to generate the $CF_3CH_2CF_2$ end group, for which the CF_3 ^{19}F NMR signal is expected at -60.1 ppm.[48] However, the identification of this chain end was prevented by the high molar mass of the recovered polymer, except for entry 3 where a very small signal at -61.4 ppm could be observed (Figure S.F.6.2), although not strong enough for integration. The high molar masses relative to the calculated values for an ideal controlled process show low initiator efficiencies (with apparent values calculated from the molar masses estimated by SEC equal to 0.19, 0.08 and 0.13 for the thermal, visible and UV methods, respectively), indicating that the thermal activation method is the most efficient one. Since the kinetic studies of the thermal decomposition (section b), backed up by the DFT calculations, clearly show that **5** has the strongest Mn-R_F BDE amongst all investigated compounds, there is little doubt that the other compounds (**6**-**8**) would also be able to function as radical initiators.

Conclusions

The new fluoroalkyl derivatives of pentacarbonylmanganese(I), $[Mn(CO)_5(R_F)]$ (R_F = CH_2CF_3, **7**; CF_2CH_3, **8**), which are models of the "head" and "tail" dormant chains of PVDF resulting from the radical chain trapping by the $[(CO)_5Mn^{\bullet}]$ radical, have been prepared and investigated. Compound **8** could not be obtained in a pure state, presumably because the homolytic Mn-CF_2CH_3 bond dissociation occurs simultaneously with its generation under the harsh thermal conditions of the acyl precursor decarbonylation. The spectroscopic characterization of compounds **1**-**8** by ^1H, ^{13}C and ^{19}F NMR provides useful and previously unavailable reference values for fluoroalkyl groups bonded to $Mn(CO)_5$. In addition, the IR properties of the alkyl complexes **5**-**7** in solution have been fully explored at un unprecedented level of detail with the assistance of DFT calculations, resulting in the full symmetry analysis of the major $[Mn(^{12}CO)_5(R_F)]$ and minor $[Mn(^{12}CO)_4(eq\text{-}^{13}CO)(R_F)]$ and $[Mn(^{12}CO)_4(ax\text{-}^{13}CO)(R_F)]$ isotopomers and in the unambiguous assignment of several observed weak bands. The experimental determination of the homolytic Mn-R_F bond cleavage activation parameters for **7** as well as for the well-known analogues with R_F = CF_3 (**5**) and CHF_2 (**6**), carried out by saturation kinetics with trapping by TTMSS, gave values in close agreement with recent DFT estimations[18] but significantly higher than previous determinations by other experimental methods.[35-36] The aptitude of these complexes to release fluoroalkyl radicals in solution was demonstrated by the successful initiation of the radical polymerization of VDF using compound **5**, which is the member with the strongest Mn-R_F bond. The PVDF was obtained in good yields both under thermal conditions in the dark at 100 °C (but not at 50 °C) and under photochemical conditions (visible or ultraviolet light) at moderate temperatures (40-50 °C). These results rationalize the lack of accumulation of $[Mn(CO)_5(PVDF)]$ dormant species in the recently reported iodine transfer polymerization of VDF assisted by $[Mn_2(CO)_{10}]$.[12]

Experimental Section

General. All operations were carried out under an atmosphere of argon except for the purifications by column chromatography, which were carried out in air, and for the sublimations and polymerizations (under vacuum, products collected in air).

Materials. Compounds $[Mn_2(CO)_{10}]$ (98%, Strem Chemicals), trifluoroacetic anhydride (ReagentPlus® grade, ≥99%, Sigma-Aldrich), difluoroacetic acid (98%, Fluorochem), 3,3,3-trifluoropropionyl chloride (98%, Fluorochem), 1-Iodo-2,2,2-trifluoroethane (97%, Fluorochem), 2,2-difluoropropionic acid (98%, Fluorochem), P_2O_5 (≥98%, Fluka), (2,2,6,6-tetramethylpiperidin-yl)oxy (TEMPO, 98%, Acros Organics), tris(trimethylsilyl)silane (TTMSS, 97%, Sigma-Aldrich), hexafluorobenzene (99%, Aldrich), benzene-D_6 (99.5%D, Euriso-top), acetone-D_6 (99.5%D, Euriso-top), DMSO-D_6 (99.5%D, Euriso-top), DMF-D_7 (99.5%D, Euriso-top), dimethyl carbonate (≥99%, Merck KGaA) and silica (40-63 µm, VMR

Chemicals) were used as received. Potassium (98%, Aldrich) and sodium (≥99.8%, Aldrich) were washed in *n*-pentane to remove the mineral oil prior to use. Laboratory Reagent grade (≥99.5%) diethyl ether, *n*-pentane and THF were purchased from Sigma-Aldrich. THF was purified by percolation through a dry activated alumina column. Thionyl chloride (ReagentPlus® grade, ≥99%, Sigma-Aldrich) was distilled in the presence of sulphur prior to use. VDF was kindly supplied by Arkema and used as received. Difluoroacetic anhydride (from difluoroacetic acid and P_2O_5)[49] and 2,2-difluoropropionyl chloride (from 2,2-difluoropropionic acid and oxalyl chloride)[50] were synthesized as described in the literature. The preparations of compounds $[Mn(COCF_3)(CO)_5]$, $[Mn(CF_3)(CO)_5]$, $[Mn(COCHF_2)(CO)_5]$, and $[Mn(CHF_2)(CO)_5]$, were adapted from the literature procedures:[19] purifications were carried out by column chromatography through a silica column, using *n*-pentane as the mobile phase to eliminate the $[Mn_2(CO)_{10}]$ impurity and then a 1:9 diethyl ether/pentane mixture to elute the product. Single crystals of $[Mn(COCF_3)(CO)_5]$, $[Mn(CF_3)(CO)_5]$, $[Mn(COCHF_2)(CO)_5]$, $[Mn(CHF_2)(CO)_5]$ and $[Mn(CH_2CF_3)(CO)_5]$ for the X-ray diffraction analysis were grown by sublimation at 50 °C and 100 mbar. Single crystals of $[Mn(COCF_2CH_3)(CO)_5]$ were obtained directly in the flask after the evaporation of the solvent in a rotary evaporator.

Instrumentation. The Nuclear Magnetic Resonance (NMR) spectra were recorded on a Bruker Avance III HD 400 MHz spectrometer. The instrumental parameters for recording spectra were as follows: ^{1}H NMR: flip angle 30°, acquisition time 5.7 s, pulse delay 2 s, number of scans 64, and a pulse width of 3.05 µs; ^{19}F NMR: flip angle 30°, acquisition time 2 s, pulse delay 2 s, number of scans 64, and a pulse width of 3.76 µs; ^{13}C NMR: flip angle 30°, acquisition time 1.5 s, pulse delay 2 s, number of scans 10240, and a pulse width of 3.27 µs. The probe has a lower background ^{19}F NMR signals compared to standard dual-channel probes. The NMR properties for all compounds are reported in Table 1 and the individual spectra are shown in the SI (part A). For the homolytic Mn-R Bond cleavage experiments, the temperature of the NMR probe was calibrated using ethylene glycol and is believed to be accurate to ± 0.05 °C. The Fourier transform infrared (FTIR) spectra on the pentane solutions were recorded in transmission mode with a PerkinElmer Spectrum One FT-IR Spectrophotometer using a CaF_2 window with a 0.05 mm optical path length. The IR properties in the CO stretching region for all compounds are collected in Table 3 and the individual spectra are shown in the SI (part C). The elemental analyses were carried out by the analytical service of the LCC-Toulouse using a PerkinElmer 2400 CHNS/O Series II System (100V). The apparent number average molar masses and dispersity (Đ) of the synthesized polymers were determined using a Varian 390-LC gel permeation chromatography (GPC) system equipped with differential refractive index (RI), light scattering (LS) and viscosity detectors using a guard column (Varian Polymer Laboratories PLGel 5µm, 50 x 7.5 mm) and two ResiPore columns of the same type. The mobile phase was DMF with 0.1% wt LiBr adjusted at a flow rate of 1 mL min^{-1} while the columns were thermostated to 70 °C. The GPC system was calibrated using narrow poly(methyl methacrylate) (PMMA) standards ranging from 550 to 1,568,000 g mol^{-1} (EasiVial- Agilent).

Synthesis of 3,3,3-trifluoropropanoyl(pentacarbonyl)manganese, 3. In a Schlenk tube, liquid "NaK" alloy was prepared from 395 mg (10.1 mmol) of metallic potassium and 260 mg (11.3 mmol) of metallic sodium under argon. A solution of dimanganese decacarbonyl (3.00 g, 7.69 mmol) in 30 mL of dry THF was added and the resulting mixture was stirred for 3 h at room temperature, with IR monitoring to verify the completion of the reduction process. The mixture was filtered through Celite to yield a greenish-brown solution, rinsing the Celite with 10 mL of dry THF. Then, 3,3,3-trifluoropropanoyl chloride (2.25 g, 15.36 mmol) was added dropwise at room temperature, generating a light red solution, which subsequently turned bright red and finally orange after 1 h. After additional stirring at room temperature (total 3 h), the solvent was evaporated under reduced pressure and the product was purified by column chromatography. A light-yellow band was collected, followed by evaporation to dryness under reduced pressure to afford the product as a pale-yellow solid (3.56 g, 11.5 mmol, yield 75%). Anal. % calcd. for $(CO)_5Mn(COCH_2CF_3)$, $C_8H_2F_3MnO_6$, C, 31.40; H, 0.66. Found, C, 31.5; H, 0.1.

Synthesis of 2,2,2-trifluoroethyl(pentacarbonyl)manganese, 7. Compound $[(CO)_5Mn(COCH_2CF_3)]$ (2.25 g, 7.35 mmol) was introduced in a two-neck flask connected to a reflux condenser to avoid any sublimation losses. The flask was then heated under normal pressure to 70°C for 1.5 h. During this time, the solid that accumulated at the bottom of the condenser was periodically removed and dropped back to the warm flask bottom. The resulting light-brown powder was purified by column chromatography, yielding the product as a yellow solid (1.63 g, 5.86 mmol, yield 80%). A single crystal for the X-ray diffraction analysis was obtained by sublimation at 55 °C and 100 mbar. The decarbonylation of $[(CO)_5Mn(COCH_2CF_3)]$ could also be accomplished by heating the solid in a sublimation apparatus under vacuum at 55 °C under 100 mbar for 5 days. Starting the reaction from 1.978 g of manganese carbonyl (5.07 mmol) and 1.473 g of 3,3,3-trifluoropropanoyl chloride (10.06 mmol) and following the same synthetic procedure, the pure product (1.122 g, 4.04 mmol, yield 40 %) was directly collected as a light yellow microcrystalline powder from the cold finger. Anal. % calcd. for $(CO)_5Mn(CH_2CF_3)$, $C_7H_2F_3MnO_5$, C, 30.24; H, 0.73. Found, C, 30.54; H, 0.83.

Synthesis of 2,2-difluoropropanoyl(pentacarbonyl)manganese, 4. The procedure was similar to that described above for the synthesis of compound 3, using K (400 mg, 10.23 mmol), Na (300 mg, 13.05 mmol), $[Mn_2(CO)_{10}]$ (3.00 g, 7.69 mmol), dry THF (30 mL), and 2,2-difluoropropanoyl chloride (1.98 g, 15.45 mmol). The latter was produced *in situ* as follows. 2,2-Difluoropropionic acid (1.70 g, 15.45 mmol) was introduced in 50 mL two-neck flask connected to a bubbler and dissolved in 5 mL of dry THF. Then oxalyl chloride (2.11 g, 16.62 mmol) was added dropwise and finally 150 µL of dry DMF was added. The mixture was stirred for 1 h (until bubbling stopped). The resulting 2,2-difluoropropanoyl chloride solution was directly added dropwise to the $K[Mn(CO)_5]$ solution at room temperature. The initially clear orange solution turned cloudy and yellow within a few minutes. After stirring at room temperature for 3 h, the solvent was evaporated under reduced pressure. The product work-up procedure was the same as for the synthesis of $[(CO)_5Mn(COCH_2CF_3)]$. The light-yellow (nearly colorless) band collected after the $[Mn_2(CO)_{10}]$ removal yielded the product as volatile brownish-white needle-shape microcrystals after solvent evaporation (1.49 g, 5.17 mmol, yield 33%). A third fraction of an orange unidentified oil was recovered immediately after that of the product. Anal. % calcd. for $[(CO)_5Mn(COCF_2CH_3)]$, $C_8H_3F_2MnO_6$, C, 33.36; H, 1.05. Found, C, 33.9; H, 0.7.

Synthesis of 1,1-difluoroethyl(pentacarbonyl)manganese, 8. Compound $[(CO)_5Mn(COCF_2CH_3)]$ (20 mg, 0.069 mmol) was introduced in a 50 mL two-neck flask and dissolved in 5 mL of 2-butanone. The system was connected to a refrigerant and to a bubbler and purge for 15 min with an argon flow. Then it was heated up to 80°C for 1 h. The solvent was finally removed by evaporation under reduced pressure leading to a yellow powder which contain the complex **8** (yield 64%, determined by relative integration of $[(CO)_5Mn(COCF_2CH_3)]$ and $[(CO)_5Mn(CF_2CH_3)]$ signals). The small amount obtained after decarbonylation reaction did not allow its purification by column chromatography. Additional experiments carried out with a greater amount of complex and heating for a longer period let to decomposition of the desired product and lower spectroscopic yields.

Investigation of the Homolytic Mn-R Bond Cleavage. All experiments were carried out using the same procedure. As a representative example, $[(CO)_5Mn(CF_3)]$ (159.3 mg, 0.60 mmol) was dissolved in 5.0 mL of C_6D_6 together with 8 drops of C_6F_6 as internal standard. Aliquots of this solution (0.4 mL) were transferred into NMR tubes, then the desired amount of $(TMS)_3SiH$ was added and the thermal decomposition was monitored at the desired temperatures by ^{19}F NMR. The signal of hexafluorobenzene (internal standard) is integrated from -162.8 ppm to -163.2 ppm, and the value of the internal standard was set to 1 in all the spectra. Then the complex signal was integrated from 7.7 ppm to 8.1 ppm. Knowing the initial concentration of complex in each tube (C_0), the concentration of complex

at time t (C_t) was determined by the as $C_t = C_0 I_t / I_0$, where I_0 and I_t stand for the integral value of the NMR signal of the complex at t = 0 and at t, respectively. The $\ln[C_0/C_t]$ *vs* time plots led to straight lines, the slopes of which represents k (Figures S.E3.1- Figure S.E3.3).

VDF polymerizations with trifluoromethyl(pentacarbonyl)manganese. The radical polymerizations of VDF were carried out in thick-walled 12 mL Carius tubes in which the solvent (5 mL of dimethyl carbonate) and $[(CO)_5Mn(CF_3)]$ (128 mg, 0.48 mmol) were added. The resulting solutions were then degassed by performing three freeze-pump-thaw cycles. Then, the gaseous VDF monomer (1.5 g, 23.4 mmol) was transferred into the Carius tube, which was cooled at the liquid nitrogen temperature, using a custom-made manifold that enables the accurate measurement of the gas quantity (using "pressure drop vs mass of monomer" calibration curve). The tube was then sealed under static vacuum at the liquid nitrogen temperature. For the thermal activation experiments, the tube was placed horizontally in a thermostatic shaking water bath while for the visible light activation experiment, it was placed horizontally in a tube roller shaker with 3 LED bulbs (Diall 1102270698, 14 W, 1521 lm), radiating from above, placed at 2 cm from the tube. The proximity of the bulbs caused the tube to warm up to ca. 40 °C. For the UV activation experiment, the tube was equipped with a small magnetic stirring bar and stirred vertically in a Rayonet RPR-200 UV reactor equipped with sixteen 300 nm wavelength UV-lamps of 35 W each. Despite the fan placed inside the UV chamber, the heat generated by the UV lamps caused the tube to warm up to ca. 50 °C. After 24 h, each tube was frozen into liquid nitrogen, opened, and the solvent was evaporated in a rotary evaporator. The resulting polymers were dissolved in deuterated DMF and analyzed by ^{1}H and ^{19}F NMR spectroscopies. The molar masses and dispersities were determined by SEC chromatography in DMF (refractive index, calibrated with PMMA standards).

Table 6. Crystal and refinement parameters for all compounds investigated by X-ray diffraction.

Identification code	**1**	**2**	**4**	**5**	**6**	**7**
Empirical formula	$C_7F_3MnO_6$	$C_7HF_2MnO_6$	$C_8H_3F_2MnO_6$	$C_6F_3MnO_5$	$C_6HF_2MnO_5$	$C_7H_2F_3MnO_5$
Formula weight	292.01	274.02	288.04	264.91	246.01	278.03
Temperature, K	173(4)	180(2)	173(2)	173(2)	173(2)	173(2)
Wavelength, Å	0.71073	0.71073	0.71073	0.71073	0.71073	0.71073
Crystal system	Orthorhombic	Orthorhombic	Monoclinic	Monoclinic	Orthorhombic	Monoclinic
Space group	$Pna2_1$	$Pna2_1$	$P2_1/c$	$P\ 2_1/m$	Pnma	$P2_1/n$
a, Å	14.4714(4)	14.0916(7)	14.6140(10)	6.3579(4)	12.2397(3)	11.6543(7)
b, Å	10.8047(4)	10.8226(7)	6.2155(4)	11.0117(6)	10.7284(2)	6.8405(4)
c, Å	6.3778(2)	6.3265(3)	12.4305(9)	6.5655(4)	6.29540(10)	24.2843(14)
α, °	90.0	90.0	90.0	90.0	90.0	90.0
B, °	90.0	90.0	106.608(2)	107.459(2)	90.0	□= 96.288(5)
γ, °	90.0	90.0	90.0	90.0	90.0	90.0
Volume, Å^3	997.23(6)	964.84(9)	1082.00(13)	438.48(5)	826.66(3)	1924.3(2)
Z	4	4	4	2	4	8
Density (calc), Mg/m^3	1.945	1.886	1.768	2.000	1.977	1.919
Abs. coefficient, mm^{-1}	1.384	1.409	1.261	1.768	1.623	1.421
F(000)	568	536	568	256	480	1088
Crystal size, mm^3	0.38 x 0.25 x 0.20	0.32 x 0.25 x 0.14	0.20 x 0.12 x 0.05	0.38 x 0.32 x 0.20	0.37 x 0.32 x 0.2	0.50 x 0.20 x 0.13
Theta range, °	3.389 to 26.342	3.450 to 26.365	1.454 to 30.029	3.253 to 27.103°.	3.329 to 26.367	3.095 to 26.372
Reflections collected	5749	5532	27995	7025	9162	10468
Indpt reflections (R_{int})	2006 (0.0257)	1777 (0.0326)	3169 (0.0317)	1021 (0.0299)	890 (0.0733)	3934 (0.0232)
Completeness, %	99.5	99.1	100.0	99.9	99.8	99.4
Absorption correction	Multi-scan	Multi-scan	Multi-scan	Multi-scan	Multi-scan	Multi-scan
Max. / min. Transm.	1.0 / 0.944	1.0 / 0.669	0.7476 / 0.6021	0.7461 / 0.5264	0.7457 / 0.6876	1.0 / 0.787
Refinement method	F^2	F^2	F^2	F^2	F^2	F^2
Data /restraints/param.	2006 / 38 / 212	1777 / 1 / 145	3169 / 0 / 155	1021 / 0 / 76	890 / 0 / 88	3934 / 0 / 289
Goodness-of-fit on F^2	1.029	1.119	1.159	1.158	1.145	1.092
R1, wR2 [I>2σ(I)]	0.0223, 0.0467	0.0405, 0.1090	0.0254, 0.0734	0.0254, 0.0640	0.0248, 0.0667	0.0279, 0.0630
R1, wR2 (all data)	0.0250, 0.0477	0.0419, 0.1107	0.0301, 0.0869	0.0264, 0.0647	0.0254, 0.0674	0.0341, 0.0662
Flack's parameter	0.067(12)	0.01(3)				
Residual density, e.Å^{-3}	0.224 / -0.172	0.947 / -0.853	0.686 / -0.450	0.493 / -0.582	0.516 / -0.582	0.323 / -0.279

X-ray crystallography. A single crystal of each compound was mounted under inert perfluoropolyether on the tip of a glass fibre and cooled in the cryostream of either a Rigaku Oxford-Diffraction Gemini EOS diffractometer (for **1**, **2** and **7**) or a Bruker APEXII diffractometer (for **4**, **5** and **6**). The structures were solved by using the integrate space-group and crystal structure determination SHELXT software[51] and refined by least-squares procedures on F^2 using SHELXL-2014.[52] The crystal and refinement parameters of all compounds are collected in Table 6 and the full list of bond distances and angles provided in SI tables (section S.B). When present, the H atoms attached to carbon atoms were introduced in the calculations at idealized positions and treated with the riding model, except for compound 6 where, because of a disorder affecting the CHF_2 group, the H atom position was refined. In three of the six compounds, namely **1**, **2** and **6**, the fluorinated organic fragments show positional disorder. In compound **1**, the CF_3 group is disordered by free rotation around the C6-C7 bond. To model the disorder, three different orientations were refined using the PART and SUMP instructions to constrain the sum of the occupancy factors, which refined to 0.46, 0.28 and 0.26, to be equal to 1. In compound **2**, the CHF_2 moiety is disordered over two positions by a ca. 36° rotation around the C1-C11 bond. To model this disorder, the PART and restrain instructions (SADI) were used. In compound 6, the mirror plane m (x, ¼, z) containing the Mn1, C2, O2, C3 and O3 atoms makes the CHF_2 group and a CO ligand share the same two sites. The absolute structures for **1** and **2** were determined by refining the Flack parameter.[53] The drawings of the molecules were realised with the help of ORTEP32.[54] Crystallographic data (excluding structure factors) have been deposited with the Cambridge Crystallographic Data Centre as supplementary publication no. CCDC 1851284-1851288. Copies of the data can be obtained free of charge on application to the Director, CCDC, 12 Union Road, Cambridge CB2 1EZ, UK (fax: (+44) 1223-336-033; e-mail: deposit@ccdc.cam.ac.uk).

Computational Details. The IR spectra of compounds **5-8** were computed using the Gaussian09 suite of programs,[55] using the previously optimized

geometries. The same level of theory previously used for the geometry optimization (BPW91* functional;[56] 6-31G(d,p) basis functions for all light atoms (H, C, F, O, S) and SDD basis set augmented by an f polarization function (α = 2.195) for the Mn atom[57]) was adopted for the ffrequency calculations for all isotopomers (see text).

Acknowledgements

This work was supported by the Agence Nationale de la Recherche (ANR, French National Agency) through the project FLUPOL (grant No. ANR-14-CE07-0012). We also gratefully acknowledge additional financial support from the Centre National de la Recherche Scientifique (CNRS). We thank Arkema (Pierre Bénite, France) for supplying free sample of VDF and Mr. Cédric Totée and Pr. Gilles Silly for their help in NMR spectroscopy. This work was granted access to the HPC resources of IDRIS under the allocation 2016-086343 made by GENCI (Grand Équipement National de Calcul Intensif) and to the resources of the CICT (Centre Interuniversitaire de Calcul de Toulouse, project CALMIP).

Keywords: bond dissociation enthalpy • fluoroalkyl radicals • manganese • radical polymerization • vinylidene fluoride

[1] R. D. Closson, J. Kozikowski and T. H. Coffield, *J. Org. Chem.* **1957**, *22*, 598-598.

[2] a) T. H. Coffield, J. Kozikowski and R. D. Closson, *J. Org. Chem.* **1957**, *22*, 598-598; b) F. Calderazzo and F. A. Cotton, *Inorg. Chem.* **1962**, *1*, 30-36.

[3] R. H. Crabtree, *The Organometallic Chemistry of the Transition Metals*, Wiley-Interscience, New York, **2005**.

[4] W. Beck, W. Hieber and H. Tengler, *Chem. Ber.* **1961**, *94*, 862-872.

[5] a) T. H. Coffield, J. Kozikowski and R. D. Closson, *Abstracts of the International Conference on Coordination Chemistry, London* **April 1959**, 126; b) H. D. Kaesz, R. B. King and F. G. A. Stone, *Z. Naturforsch. B* **1960**, *15*, 763-764.

[6] a) F. Calderazzo, K. Noack and U. Schaerer, *J. Organomet. Chem.* **1966**, *6*, 265-271; b) K. Noack, U. Schaerer and F. Calderazzo, *J. Organometal. Chem.* **1967**, *8*, 517-526.

[7] D. Naumann and M. Kaiser, *Z. Anorg. Allg. Chem.* **1995**, *621*, 812-816.

[8] a) X. Ma, Z. Zuo, G. Liu and Z. Huang, *ACS Omega* **2017**, *2*, 4688-4692; b) D. A. Valyaev, D. Wei, S. Elangovan, M. Cavailles, V. Dorcet, J.-B. Sortais, C. Darcel and N. Lugan, *Organometallics* **2016**, *35*, 4090-4098; c) S. Vijjamarri, V. K. Chidara and G. Du, *ACS Omega* **2017**, *2*, 582-591.

[9] a) N. Duc Hanh, X. Trivelli, F. Capet, J.-F. Paul, F. Dumeignil and R. M. Gauvin, *ACS Catal.* **2017**, *7*, 2022-2032; b) B. Dutta, V. Sharma, N. Sassu, Y. Dang, C. Weerakkody, J. Macharia, R. Miao, A. R. Howell and S. L. Suib, *Green Chem.* **2017**, *19*, 5350-5355; c) N. A. Espinosa-Jalapa, A. Kumar, G. Leitus, Y. Diskin-Posner and D. Milstein, *J. Am. Chem. Soc.* **2017**, *139*, 11722-11725.

[10] W. Liu and L. Ackermann, *ACS Catal.* **2016**, *6*, 3743-3752.

[11] D. Zell, U. Dhawa, V. Mueller, M. Bursch, S. Grimme and L. Ackermann, *ACS Catal.* **2017**, *7*, 4209-4213.

[12] a) A. D. Asandei, O. I. Adebolu and C. P. Simpson, *J. Am. Chem. Soc.* **2012**, *134*, 6080-6083; b) C. P. Simpson, O. I. Adebolu, J.-S. Kim, V. Vasu and A. D. Asandei, *Macromolecules* **2015**, *48*, 6404-6420.

[13] a) M. Tatemoto, *Int. Polym. Sci. Tech.* **1985**, *12*, 85-98; b) G. David, C. Boyer, J. Tonnar, B. Améduri, P. Lacroix-Desmazes and B. Boutevin, *Chem. Rev.* **2006**, *106*, 3936-3962; c) S. Banerjee, Y. Patil, T. Ono and B. Améduri, *Macromolecules* **2017**, *50*, 203-214.

[14] a) M. A. Bachmann, W. L. Gordon, J. L. Koenig and J. B. Lando, *Journal of Applied Physics* **1979**, *50*, 6106-6112; b) D. E. Mattern, F. T. Lin and D. M. Hercules, *Analytical Chemistry* **1984**, *56*, 2762-2769; c) A. J. Lovinger, D. D. Davis, R. E. Cais and J. M. Kometani, *Polymer* **1987**, *28*, 617-626; d) P. Pladis, A. H. Alexopoulos and C. Kiparissides, *Ind. Engin. Chem. Res.* **2014**, *53*, 7352-7364.

[15] A. D. Asandei, *Chem. Rev.* **2016**, *116*, 2244-2274.

[16] a) R. Poli, *Angew. Chem. Int. Ed.* **2006**, *45*, 5058–5070; b) R. Poli in *Organometallic Mediated Radical Polymerization*, *Vol. 3* Eds.: K. Matyjaszewski and M. Möller), Elsevier BV, Amsterdam, **2012**, pp. 351–375; c) R. Poli, *Chem. Eur. J.* **2015**, *21*, 6988-7001.

[17] a) J. Demarteau, B. Améduri, V. Ladmiral, M. A. Mees, R. Hoogenboom, A. Debuigne and C. Detrembleur, *Macromolecules* **2017**, *50*, 3750-3760; b) S. Banerjee, E. V. Bellan, F. Gayet, A. Debuigne, C. Detrembleur, R. Poli, B. Améduri and V. Ladmiral, *Polymers* **2017**, *9*, 802; c) S. Banerjee, V. Ladmiral, A. Debuigne, C. Detrembleur, S. M. W. Rahaman, R. Poli and B. Améduri, *Macromol. Rapid Commun.* **2017**, *38*, 1700203; d) S. Banerjee, V. Ladmiral, A. Debuigne, C. Detrembleur, R. Poli and B. Améduri, *Angew. Chem. Int. Ed.* **2018**, *57*, 2934–2937.

[18] R. Poli, S. M. W. Rahaman, V. Ladmiral and B. Améduri, *J. Organomet. Chem.* **2018**, *864*, 12-18

[19] a) R. B. King in *Alkyl, Acyl and perfluoroalkyl metal carbonyls*, *Vol. 1* Academic Press, NY, **1965**, pp. 145-147; b) R. B. King, *Acc. Chem. Res.* **1970**, *3*, 417-427.

[20] J. E. Ellis and E. A. Flom, *J. Organomet. Chem.* **1975**, *99*, 263-268.

[21] a) R. B. King, *J. Inorg. Nucl. Chem.* **1963**, *25*, 1296-1298; b) J. J. Eisch and R. B. King, *Organometallic syntheses*, Academic Press, New York and London, **1965**; c) R. B. King and F. G. A. Stone, *Inorg. Synth.* **1963**, *7*, 196-201.

[22] F. Calderazzo, E. A. C. Lucken and D. F. Williams, *J. Chem. Soc. A* **1967**, 154-158.

[23] S. Evans, J. C. Green, M. L. H. Green, A. F. Orchard and D. W. Turner, *Discussions of the Faraday Society* **1969**, 112-120.

[24] a) F. W. Einstein, H. Luth and J. Trotter, *J. Chem. Soc. A* **1967**, 89-93; b) R. P. Hughes, S. J. Doig, R. C. Hemond, W. L. Smith, R. E. Davis, S. M. Gadol and K. D. Holland, *Organometallics* **1990**, *9*, 2745-2753; c) D. Lentz and S. Willemsen, *Angew. Chem. Int. Ed.* **2001**, *40*, 2087-2091; d) M. F. Kuehnel and D. Lentz, *Dalton Trans.* **2009**, 4747-4755.

[25] A. P. Masters, J. F. Richardson and T. S. Sorensen, *Canad. J. Chem.* **1990**, *68*, 2221-2227.

[26] E. Lindner, W. Wassing, R. Fawzi and M. Steimann, *Z. Natuforsch. B* **1993**, *48*, 1651-1660.

[27] M. A. Andrews, J. Eckert, J. A. Goldstone, L. Passell and B. Swanson, *J. Am. Chem. Soc.* **1983**, *105*, 2262-2269.

[28] B. K. Nicholson, J. S. McIndoe, D. A. Clemente and W. T. Robinson, *Structural Chemistry* **2008**, *19*, 489-492.

[29] F. A. Cotton, A. Musco and G. Yagupsky, *Inorg. Chem.* **1967**, *6*, 1357-1364.

[30] S. C. Tenhaeff, K. J. Covert, M. P. Castellani, J. Grunkemeier, C. Kunz, J. R. Weakley, T. Koenig and D. R. Tyler, *Organometallics* **1993**, *12*, 5000-5004.

[31] a) R. G. Finke and B. P. Hay, *Inorg. Chem.* **1984**, *23*, 3041-3043; b) J. Halpern, S. H. Kim and T. W. Leung, *J. Am. Chem. Soc.* **1984**, *106*, 8317-8319.

[32] a) G. N. Schrauzer and J. H. Grate, *J. Am. Chem. Soc.* **1981**, *103*, 541-546; b) R. J. Blau and J. H. Espenson, *J. Am. Chem. Soc.* **1985**, *107*, 3530-3533; c) S. H. Kim, H. L. Chen, N. Feilchenfeld and J. Halpern, *J. Am. Chem. Soc.* **1988**, *110*, 3120-3126.

[33] a) A. Goto and T. Fukuda, *Macromol. Rapid Commun.* **1999**, *20*, 633-636; b) K. Matyjaszewski, H.-j. Paik, P. Zhou and S. J. Diamanti, *Macromolecules* **2001**, *34*, 5125-5131; c) A. K. Nanda and K. Matyjaszewski, *Macromolecules* **2003**, *36*, 8222-8224; d) T. Pintauer, W. Braunecker, E. Collange, R. Poli and K. Matyjaszewski, *Macromolecules* **2004**, *37*, 2679-2682.

[34] T. J. Meyer and J. V. Caspar, *Chem. Rev.* **1985**, *85*, 187-218.

[35] J. A. Connor, M. T. Zafaranimoattar, J. Bickerton, N. I. Elsaied, S. Suradi, R. Carson, G. Altakhin and H. A. Skinner, *Organometallics* **1982**, *1*, 1166-1174.

[36] J. A. Martinho Simões and J. L. Beauchamp, *Chem. Rev.* **1990**, *90*, 629-688.

[37] Y. Zhu, J. Gong and Y. Wan, *J. Org. Chem.* **2017**, *82*, 7428-7436.

[38] a) P. Jaitner, W. Huber, G. Huttner and O. Scheidsteger, *J. Organomet. Chem.* **1983**, *259*, C1-C5; b) D. Rehder and P. Jaitner, *J. Organomet. Chem.* **1987**, *329*, 337-342; c) J. P. Lomont, S. C. Nguyen and C. B. Harris, *J. Am. Chem. Soc.* **2013**, *135*, 11266-11273.

[39] a) C. Chatgilialoglu, D. Griller and M. Lesage, *J. Org. Chem.* **1988**, *53*, 3641-3642; b) M. Ballestri, C. Chatgilialoglu, K. B. Clark, D. Griller, B. Giese and B. Kopping, *J. Org. Chem.* **1991**, *56*, 678-683.

[40] a) C. Chatgilialoglu, D. Griller and M. Lesage, *J. Org. Chem.* **1989**, *54*, 2492-2494; b) C. Chatgilialoglu, J. Dickhaut and B. Giese, *J. Org. Chem.* **1991**, *56*, 6399-6403; c) C. Chatgilialoglu, *Helv. Chim. Acta* **2006**, *89*, 2387-2398.

[41] M. Ishikawa, A. Nakamura and M. Kumada, *J. Organometal. Chem.* **1973**, *59*, C11-C12.

[42] a) B. K. Nicholson and J. Simpson, *J. Organometal. Chem.* **1971**, *32*, C29-C30; b) B. K. Nicholson, J. Simpson and W. T. Robinson, *J. Organometal. Chem.* **1973**, *47*, 403-412.

[43] D. K. Russell, I. M. T. Davidson, A. M. Ellis, G. P. Mills, M. Pennington, I. M. Povey, J. B. Raynor and S. Saydam, *Chem. Vap. Deposition* **1998**, *4*, 103-107.

[44] E. Folga and T. Ziegler, *J. Am. Chem. Soc.* **1993**, *115*, 5169-5176.

[45] J. Guiot, B. Ameduri and B. Boutevin, *Macromolecules* **2002**, *35*, 8694-8707.

[46] a) M. Pianca, E. Barchiesi, G. Esposto and S. Radice, *J. Fluorine Chem.* **1999**, *95*, 71-84; b) M. Destarac, K. Matyjaszewski, E. Silverman, B. Améduri and B. Boutevin, *Macromolecules* **2000**, *33*, 4613-4615; c) E. Girard, J. D. Marty, B. Améduri and M. Destarac, *ACS Macro Lett.* **2012**, *1*, 270-274; d) N. Golzari, J. Adams and S. Beuermann, *Polymers* **2017**, *9*.

[47] S. M. Aliwi, C. H. Bamford and S. U. Mullik, *J. Polym. Sci., Polym. symp.* **1975**, 33-50.

[48] a) B. Ameduri, C. Ladaviere, F. Delolme and B. Boutevin, *Macromolecules* **2004**, *37*, 7602-7609; b) F. Boschet, T. Ono and B. Ameduri, *Macromol. Rapid Comm.* **2012**, *33*, 302-308; c) A. D. Asandei, O. I. Adebolu, C. P. Simpson and J.-S. Kim, *Angew. Chem. Int. Ed.* **2013**, *52*, 10027-10030.

[49] E. Sawicki, *J. Org. Chem.* **1956**, *21*, 376-376.

[50] B. K. Albrecht, J. E. Audia, L. A. Dakin, M. Duplessis, V. S. Gehling, J.-C. Harmange, C. G. Nasveschuk and R. G. Vaswani, *WO 2015/023915 A1* **2015**.

[51] G. M. Sheldrick, *Acta Crystallogr. A* **2015**, *71*, 3-8.

[52] G. M. Sheldrick, *Acta Crystallogr. C* **2015**, *71*, 3-8.

[53] H. D. Flack, *Acta Cryst.* **1983**, *A39*, 876-881.

[54] a) M. N. Burnett and C. K. Johnson, *ORTEPIII, Report ORNL-6895.* , Oak Ridge National Laboratory, Oak Ridge, Tennessee, U.S. , **1996**, p; b) L. J. Farrugia, *J. Appl. Cryst.* **1997**, *30*, 565.

[55] M. J. Frisch, G. W. Trucks, H. B. Schlegel, G. E. Scuseria, M. A. Robb, J. R. Cheeseman, G. Scalmani, V. Barone, B. Mennucci, G. A. Petersson, H. Nakatsuji, M. Caricato, X. Li, H. P. Hratchian, A. F. Izmaylov, J. Bloino, G. Zheng, J. L. Sonnenberg, M. Hada, M. Ehara, K. Toyota, R. Fukuda, J. Hasegawa, M. Ishida, T. Nakajima, Y. Honda, O. Kitao, H. Nakai, T. Vreven, J. Montgomery, J. A., J. E. Peralta, F. Ogliaro, M. Bearpark, J. J. Heyd, E. Brothers, K. N. Kudin, V. N. Staroverov, R. Kobayashi, J. Normand, K. Raghavachari, A. Rendell, J. C. Burant, S. S. Iyengar, J. Tomasi, M. Cossi, N. Rega, N. J. Millam, M. Klene, J. E. Knox, J. B. Cross, V. Bakken, C. Adamo, J. Jaramillo, R. Gomperts, R. E. Stratmann, O. Yazyev, A. J. Austin, R. Cammi, C. Pomelli, J. W. Ochterski, R. L. Martin, K. Morokuma, V. G. Zakrzewski, G. A. Voth, P. Salvador, J. J. Dannenberg, S. Dapprich, A. D. Daniels, Ö. Farkas, J. B. Foresman, J. V. Ortiz, J. Cioslowski and D. J. Fox, *Gaussian 09, Revision D.01*, Gaussian, Inc., Wallingford CT, **2009**, p.

[56] M. Reiher, *Inorg. Chem.* **2002**, *41*, 6928-6935.

[57] A. W. Ehlers, M. Böhme, S. Dapprich, A. Gobbi, A. Hoellwarth, V. Jonas, K. F. Koehler, R. Stegmann, A. Veldkamp and G. Frenking, *Chem. Phys. Lett.* **1993**, *208*, 111-114.

FULL PAPER

[$Mn(CO)_5(R_F)$] complexes with floroalkyl groups that model PVDF dormant chains, though having a homolytically strong Mn-R_F bond, are efficient initiators for the radical polymerization of VDF under thermal and photochemical conditions.

Roberto Morales-Cerrada, Christophe Fliedel, Jean-Claude Daran, Florence Gayet, Vincent Ladmiral, Bruno Améduri, Rinaldo Poli **

Page No. – Page No.

Fluoroalkyl radical generation by homolytic bond dissociation in pentacarbonylmanganese derivatives